

HUT Fully Polarimetric Calibration Standard for Microwave Radiometry

Janne Lahtinen, *Student Member, IEEE*, and Martti T. Hallikainen, *Fellow, IEEE*

Abstract—This paper describes the Helsinki University of Technology's Fully Polarimetric Calibration Standard (FPCS). The developed standard generates a complete Stokes reference vector and it is applied for the end-to-end absolute calibration of a fully polarimetric microwave radiometer at 36.5 GHz. The FPCS is based on the function principle of a Gasiewski–Kunkee linearly polarized (tripolarimetric) standard, with an additional phase retardation plate to generate the fourth Stokes parameter. Design considerations and operational aspects of the standard are discussed in this paper. An advanced calibration procedure, which takes advantage of both the tripolarimetric and fully polarimetric calibration scenes to suppress calibration uncertainties, is introduced. The feasibility of the standard has been verified and the generated brightness temperatures in a sample calibration are presented. An extensive set of tests has been performed to evaluate the characteristics and performance of the calibration standard. Furthermore, the use of the advanced calibration procedure to measure the characteristics of the phase retardation plate has been successfully demonstrated. The achievable calibration accuracy is analyzed and discussed relative to requirements for maritime wind vector measurements; the results indicate that the pixel-to-pixel retrieval of the wind speed is possible with high accuracy and the retrieval of the wind direction with at least moderate accuracy. In addition to calibration of a fully polarimetric radiometer, other potential applications, e.g., linearity measurements, are discussed.

Index Terms—Calibration, dielectric devices, microwave radiometry, polarimetry, remote sensing, wind.

I. INTRODUCTION

DURING THE LAST decade there has been an increasing interest in passive polarimetric microwave remote sensing. The polarimetric technique is based upon the detection of additional Stokes parameters beyond conventional vertical and horizontal polarizations. Using modified Stokes parameters [1], which are commonly used to characterize radiation components in remote sensing applications, the first (T_v) and second (T_h) parameter describe, respectively, the vertically and horizontally polarized brightness temperatures, whereas the third (T_3) and fourth (T_4) Stokes parameters describe, respectively, linearly and circularly polarized components.

Manuscript received October 3, 2001; revised September 7, 2002. This work was supported in part by the National Technology Agency of Finland (Tekes) under Contract 40266/97 and Contract 40206/98, the Graduate School in Electronics, Telecommunication and Automation (GETA), the Jenny and Antti Wihuri Foundation, the Vilho, Yrjö and Kalle Väisälä Foundation, and the Foundation of Technology.

J. Lahtinen was with the Laboratory of Space Technology, Helsinki University of Technology, 02015 HUT, Finland. He is now with the European Space Agency, ESTEC, TOS-ETP, 2200 AG Noordwijk ZH, The Netherlands (e-mail: janne.lahtinen@esa.int).

M. T. Hallikainen is with the Laboratory of Space Technology, Helsinki University of Technology, 02015 HUT, Finland.

Digital Object Identifier 10.1109/TGRS.2003.810206

One of the most promising applications of polarimetric microwave remote sensing is to retrieve both speed and direction components of maritime surface winds (e.g., see [2]–[5]). Compared to the fourth Stokes parameter, so far the use of the third Stokes parameter has been studied more extensively. However, some radiometer measurements of the fourth Stokes parameter have been carried out [3], [5]. The measurement of the fourth Stokes parameter is potentially beneficial for various remote sensing applications, including the vertical sounding of the mesosphere [6] and the retrieval of maritime wind vectors [3], [5]. Polarimetric wind vector measurements from satellite would also benefit from the immunity of the fourth Stokes parameter to Faraday rotation.

Helsinki University of Technology (HUT), Laboratory of Space Technology has developed a multichannel airborne radiometer system HUTRAD [7], which includes a direct correlating Fully Polarimetric Radiometer at 36.5 GHz [8]. Analog correlators are applied to directly correlate the orthogonally polarized field components in-phase and quadrature to measure the third and fourth Stokes parameters, respectively [9]. Compared to a nonpolarimetric radiometer, an accurate absolute calibration of such a polarimetric radiometer requires some additional hardware beyond the conventional two-point blackbody calibration targets [10].

This paper presents the HUT Fully Polarimetric Calibration Standard (FPCS), which was developed to provide an external end-to-end absolute calibration for the Fully Polarimetric Radiometer. Comprehensive tests are also included to accurately define the parameters of the device. We note that a similar fully polarimetric calibration standard was also developed at the U.S. National Oceanic and Atmospheric Administration's Environmental Technology Laboratory (NOAA/ETL) [10]. However, different requirements set for the FPCS and the partly experimental nature of the NOAA standard led to substantial differences between these two standards, both in design and characteristics. The differences in the design requirements included, e.g., frequency, aperture size, the pointing angle of the antenna, the minimum number of operating personnel, and calibration accuracy.

The FPCS was introduced in [11]. This paper presents a detailed description of the device, its use, and characteristics. We begin with a description of the hardware in Section II. The calibration procedure is presented in Section III, and calibration algorithms and associated error analysis are discussed. Section IV describes the laboratory demonstration and the measurements used to determine the characteristics of the standard; calibration uncertainties and the feasibility of the system for polarimetric

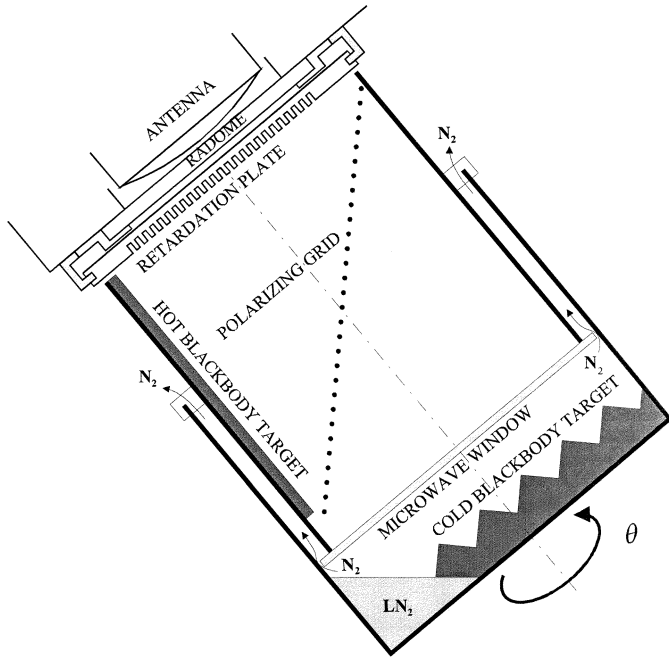


Fig. 1. Schematic diagram of the FPCS. The microwave window and U-rails for the attachment of the retardation plate are indicated using light gray; the blackbody targets are indicated using dark gray.

wind vector radiometry are also studied. Conclusions are presented in Section V.

II. EQUIPMENT

The HUT Fully Polarimetric Radiometer [8] was developed primarily for airborne measurements but can also be used for ground-based and laboratory measurements. To calibrate the instrument, the FPCS is applied prior to and after a measurement (flight). The radiometer applies Dicke switching and long-term gain variations could therefore lead to significant measurement errors during a typical calibration interval of two to three hours. As a result of efficient temperature stabilization and the careful design of the receiver, however, the radiometer has been shown to have excellent stability over comparable time scales [8]; no calibration during a measurement (flight) is thus necessary.

A schematic diagram of the FPCS is illustrated in Fig. 1. Two blackbody targets at different physical temperatures and a free-standing wire-grid polarizer form a linearly polarized standard, similar to [12]. By rotating the linearly polarized standard over angle θ about the antenna polarization basis, a variety of orthogonally and linearly polarized reference brightness temperatures are generated. It is defined that when $\theta = 0^\circ$ the wire orientation of the grid is parallel with the vertical axis of the antenna. An additional retardation plate transforms a part of the linearly polarized reference signal (third Stokes parameter) into a circularly polarized signal (fourth Stokes parameter) when positioned in the RF path between the linearly polarized standard and the radiometer antenna. A thorough analysis of the function principle of fully polarimetric calibration standards has been presented in [10].

The FPCS applies blackbody targets at ambient and nitrogen boiling temperatures, which has the following advantages:

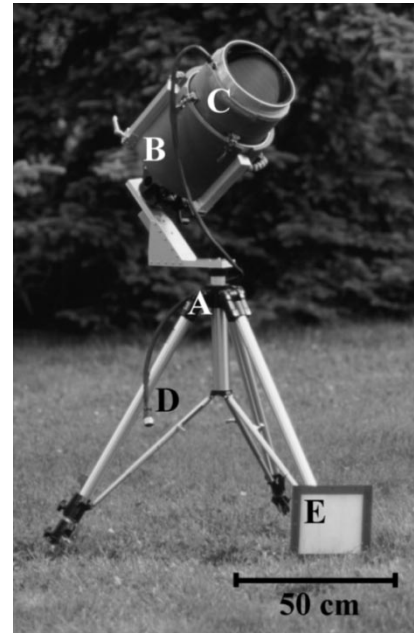


Fig. 2. FPCS. (A) Pedestal, (B) cold target subsystem, (C) hot target subsystem, (D) temperature sensor connection to the data system of the HUTRAD, and (E) retardation plate.

- 1) generated temperature difference is large (~ 200 K), which reduces error in extrapolating the calibration curve;
- 2) produced orthogonal and polarimetric brightness temperatures encompass the full range of expected earth scene temperatures;
- 3) calibration system is independent of auxiliary electrical power.

However, the use of liquid nitrogen leads to water condensation in mechanical structures of the standard. Therefore, only corrosion-free materials were used.

The varied use of the Fully Polarimetric Radiometer for airborne, ground-based (e.g., rooftop), and laboratory measurements sets requirements for the versatility of the calibration standard. On the other hand, the number of calibration personnel is often limited in measurement campaigns and the personnel may be changed. As a consequence, in addition to calibration accuracy and cost, ergonomics was an important consideration in the design of the FPCS; ease of transport, ease of mobilization, and operation by a minimum number of personnel were set as design goals. The FPCS is designed to be modular, which enables the subsystems to be transported and carried individually. If necessary, a single person can move, prepare, and operate the standard; the total weight of the FPCS is 28 kg, with the heaviest subsystem weighing 15 kg. A photograph of the FPCS is presented in Fig. 2. The calibration standard comprises four subsystems: hot target subsystem, cold target subsystem, phase retardation plate, and pedestal. Details of each of the subsystems are presented below.

A. Hot Target Subsystem

The hot target subsystem includes a blackbody target and a freestanding, polarization-splitting metal wire grid; both are housed in an aluminum cylinder 265 mm in diameter (Fig. 1). The grid is fabricated from 100- μm molybdenum wire, and it

has a bandwidth far beyond that of the radiometer [13]. The grid is estimated to be an almost ideal polarizer up to 100 GHz; at 37.5 GHz, the transmittivity was measured to be over 99% with the electric field being perpendicular to the wire orientation [13]. To reduce temperature fluctuations, the aluminum cylinder is shrouded in a jacket made of extruded polyethylene. A microwave window is attached on the bottom of the cylinder.

The hot blackbody target is a sheet of 10-mm-thick microwave absorber attached to the inner surface of the aluminum cylinder. A relatively thin flat absorber was selected due to its more suitable mechanical and thermal characteristics compared to thicker convoluted absorbers, which are often preferred as microwave blackbody targets.

For practical reasons the temperature of the hot target is uncontrolled during calibration; closeness to the cold target leads to thermal gradients across the target and to temporal variations in the physical temperature. Therefore, the temperature of the hot target is continuously monitored using three precision platinum resistive temperature detectors embedded in the absorber. Connected to the temperature measurement system of the radiometer [8], the measured physical temperatures are recorded and applied in postprocessing. Different weighting coefficients are assigned to individual temperature detectors to calculate a representative physical temperature of the hot target.

B. Cold Target Subsystem

The cold target subsystem consists of an aluminum container 300 mm in diameter and a highly absorbing, convoluted microwave absorber (Fig. 1). The container is shrouded in an extruded polyethylene jacket, which provides thermal isolation. The absorber is cooled uniformly by embedding it in liquid nitrogen prior to calibration; the boiling temperature of nitrogen (77.4 K) gives an accurate estimate of the brightness temperature of the target [14]. After the temperature has been stabilized, the surplus nitrogen is removed, and the hot target subsystem is mounted inside the cold target subsystem; when combined, these two subsystems form a linearly polarized standard.

The condensation of moisture and the formation of ice in the blackbody/air interface are a potential error source when nitrogen-cooled blackbody targets are applied. The condensation can be prevented by keeping the blackbody target completely immersed in liquid nitrogen during calibration. This, however, can cause reflections due to impedance discontinuity at the air/nitrogen interface [15]. Furthermore, in our case, the immersing during calibration is not possible for practical reasons: The target is in 50° angles during calibration, as is illustrated in Fig. 1. Therefore, the FPCS is equipped with a microwave window, which prevents the formation of ice onto the cold blackbody target. The window was cut from a sheet of low-loss extruded polyethylene and attached to the bottom of the aluminum cylinder of the hot target subsystem. The window is dimensioned to have the cold target tightly enclosed during calibration; the boil-off pressure of nitrogen gas keeps the enclosed space air-free, thus preventing the condensation of water. Another important function of the window is to reduce heat leak via convection and infrared radiation. The brightness temperature contribution of the microwave window was measured to be negligible at 36.5 GHz, far less than 0.1 K.

C. Retardation Plate

The retardation plate of the FPCS is a dielectric slab with parallel grooves machined on one face. The group velocities of transmitted electromagnetic waves parallel and perpendicular to the grooves are different, which generates a phase shift between the two polarizations [16]. The grooves of our plate were dimensioned using (1)–(3), based on [17]

$$d = \frac{c_0 \cdot \zeta}{360^\circ \cdot f \cdot (n_x - n_y)} \quad (1)$$

$$n_x = \sqrt{\frac{t_1 \varepsilon_1 + t_2 \varepsilon_2}{t_1 + t_2}} \quad (2)$$

$$n_y = \sqrt{\frac{\varepsilon_1 \varepsilon_2 (t_1 + t_2)}{\varepsilon_1 t_2 + \varepsilon_2 t_1}} \quad (3)$$

where d is the depth of the grooves; f is applied frequency; ζ is desired phase shift; c_0 is the speed of light in free space; t_1 is the width of the ridges between the grooves; t_2 is the width of the grooves; and ε_1 and ε_2 are the real parts of the relative permittivities of bulk dielectric material and air, respectively.

The development of the FPCS retardation plate was a trade-off between several factors, e.g., mechanical and electrical properties in selecting the material, and generated reflection coefficients and phase shift in selecting the groove dimensions. Cross-linked polystyrene (generally known by its market name Rexolite) was selected as the material due to its superior machinability, low loss, and relatively high permittivity ($\tan \delta = 1.0 \cdot 10^{-4}$ and $\varepsilon_1 = 2.547$ at 36.5 GHz [18]).

The theoretical power reflection of the plate is on the order of 0.4%, both in parallel with and perpendicular to the grooves. The theoretical phase shift is 37.0°, and the theoretical insertion loss is 1.011 (= 0.05 dB) and 1.008 (= 0.03 dB) in parallel with (L_{\parallel}) and perpendicular to (L_{\perp}) the grooves, respectively. The calibration errors due to phase shift variations over the radiometer bandwidth, discussed in [10], were calculated to remain negligible in this phase shift region.

In order to facilitate the use of the retardation plate, it is mounted in a plastic frame, which can be attached in front of the antenna with a high degree of precision. Two different alignments can be selected: firstly, with the plate grooves in parallel and secondly, with them perpendicular to the vertical polarization of the antenna, with the corresponding rotation angle values of $\varphi = 0^\circ$ and $\varphi = 90^\circ$, respectively. A more comprehensive technical analysis of the fabricated retardation plate is presented in [19].

D. Pedestal

The pedestal of the FPCS is a modified heavy-duty photographic tripod. During calibration the combination of hot and cold target subsystems, which equals the linearly polarized standard, is mounted on the pedestal using a three-arm clamping mechanism. An integrated pan-head enables a stepless rotation of the linearly polarized standard about the antenna polarization basis over θ ; the rotation angle is indicated precisely with a laser pointer.

III. CALIBRATION

A. Theoretical Background

The external calibration methods of microwave radiometers rely on the observations of precisely known brightness temperature scenes. Solving the relationship between the antenna temperature and the response of a (linear) radiometer enables the retrieval of the brightness temperature of any measured target. A comprehensive analysis of the calibration of fully polarimetric radiometers is presented in [10]; a short overview of the theory is given in the following.

The relation between the antenna temperature of a fully polarimetric radiometer and its output response vector is manifested by a four-element offset vector \bar{o} and a 4×4 -element gain matrix \bar{g} . The off-diagonal elements of \bar{g} represent interchannel crosstalk. Estimates of the unknown gain and offset elements can be determined via fully polarimetric calibration, which requires the generation of at least five linearly independent brightness temperature vectors. Redundant scenes can be applied to suppress random calibration uncertainties; in this case, the elements of the unknown gain-offset estimate matrix can be found using pseudoinversion, provided that the uncertainties in determining the brightness temperatures *a priori* are small enough, i.e.,

$$[\bar{g} \quad \bar{o}]^T = \left(\bar{C}_0^T \bar{C}_0 \right)^{-1} \bar{C}_0^T \bar{r}_C \quad (4)$$

where \bar{r}_C is an $M \times 4$ -size radiometer signal output matrix in calibration, and M is the number of the applied brightness temperature scenes in calibration. Stokes vector matrix \bar{C}_0 is a $M \times 5$ -size matrix containing the values of the generated brightness temperatures determined *a priori*, augmented with a unity column vector. In determining the brightness temperatures *a priori*, the following parameters are accounted for: the brightness temperatures of the hot (T_{HOT}) and cold (T_{COLD}) targets, the characteristics of the polarizing grid, the rotation angle of the linearly polarized target (θ), and the phase shift (ζ), physical temperature (T_R), rotation angle (φ), and losses (L_{\parallel} and L_{\perp}) of the retardation plate.

B. Calibration Procedure

The human factor is often nonnegligible with manually operated calibration systems. As the use of a fully polarimetric calibration standard is somewhat more cumbersome than that of conventional blackbody targets, care must be taken. To avoid flaws, minimize susceptibility to operating personnel, and reduce temporal variations, a standardized calibration procedure is followed when using the FPCS.

The antenna of the radiometer is illuminated using three distinct rotation angles of the linearly polarized target: $\theta \approx 0^\circ$, $\theta \approx 45^\circ$, and $\theta \approx 90^\circ$. Mounting the retardation plate in front of the antenna, the plate grooves in parallel with and perpendicular to the vertical polarization of the antenna at each of the three values of θ , six fully polarimetric calibration scenes are obtained. Three additional (tri-) polarimetric calibration scenes are generated when the retardation plate is removed from the

RF path. These additional scenes can be used to determine the calibration parameters of the third Stokes parameter (except the cross-talk with the fourth Stokes parameter) with enhanced accuracy. Furthermore, comparing the tripolarimetric and fully polarimetric brightness temperature scenes allows the determination of the characteristics of the retardation plate. After the generation of the tripolarimetric calibration schemes at $\theta \approx 0^\circ$ and $\theta \approx 90^\circ$, the antenna is illuminated with values of θ that deviate $\approx \pm 2^\circ$ and $\pm 4^\circ$ from the original ones; these measurements are applied in postprocessing to calibrate θ with respect to antenna polarization basis. To control the possible brightness temperature increase of the cold target, the first calibration configuration is repeated at the end.

Conventional two-point calibrations are performed prior to and after the use of the FPCS with blackbody targets at ambient (hot target) and boiling nitrogen (cold target) temperatures. As the cold calibration is especially sensitive to flaws, the two-point calibration is repeated six times to improve reliability: three times prior to and three times after the use of the FPCS. Note that the calibration parameters of the vertical and horizontal channels of the Fully Polarimetric Radiometer can be defined by the conventional calibration using the *a priori* knowledge of the low polarization cross-talk of the orthogonal channels [8].

The remaining unknown elements of the gain-offset matrix are determined using fully polarimetric calibration, which requires the generation of five linearly independent brightness temperature scenes [10]. We use, however, six fully polarimetric and two unpolarized scenes; the observation matrix \bar{C}_0 in (4) is overdetermined, and the random calibration uncertainties are suppressed.

C. Accuracy

Calibration errors are of fundamental importance in considering the absolute accuracy of a radiometer. Provided that the calibration is performed carefully and no flaws exist, the calibration errors are mostly generated by inaccuracies in determining the brightness temperatures of calibration standards *a priori*.

Assuming that the receiver noise uncertainty is made negligible by sufficiently long integration times, the uncertainties in the scene Stokes vectors as a result of calibration uncertainties are [10]

$$\begin{aligned} \Delta \bar{T}_B^T &= -\bar{C}_{B,0} [\bar{\delta g} \quad \bar{\delta o}]^T \left(\bar{g}^T \right)^{-1} \\ &\approx -\bar{C}_{B,0} \left(\bar{C}_0^T \bar{C}_0 \right)^{-1} \bar{C}_0^T \Delta \bar{T}_C^T \end{aligned} \quad (5)$$

where $\bar{C}_{B,0}$ in a fully polarimetric case is an $M \times 5$ -size scene brightness matrix acquired during operation augmented with a unity column vector. The uncertainties of the gain estimate matrix and offset estimate vector are denoted by $\bar{\delta g}$ and $\bar{\delta o}$, respectively. Matrix $\Delta \bar{T}_C^T$ contains the Stokes vector uncertainties in calibration, and the elements are functions of uncertainties associated with individual calibration standard parameters.

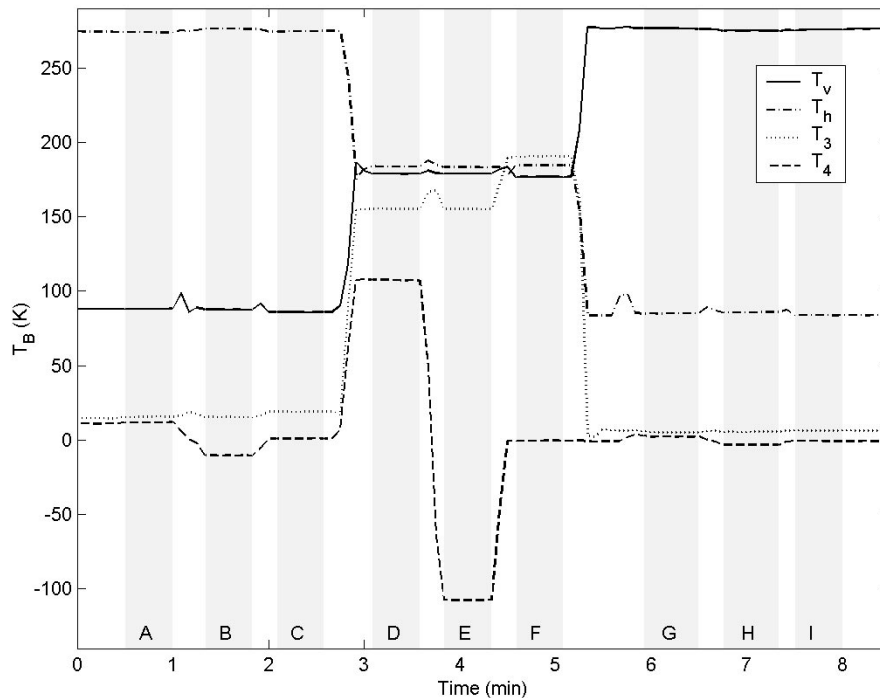


Fig. 3. Calibration demonstration. Tri- and fully polarimetric brightness temperature scenes are generated as a function of time. The data points applied in postprocessing are indicated using dark vertical bars. The following target parameters were used: (A) $\theta = 87.2^\circ$, $\varphi = 0.7^\circ$; (B) $\theta = 87.2^\circ$, $\varphi = 90.7^\circ$; (C) $\theta = 87.2^\circ$, no retardation plate; (D) $\theta = 45.6^\circ$, $\varphi = 0.7^\circ$; (E) $\theta = 45.6^\circ$, $\varphi = 90.7^\circ$; (F) $\theta = 45.6^\circ$, no retardation plate; (G) $\theta = 1.1^\circ$, $\varphi = 0.7^\circ$; (H) $\theta = 1.1^\circ$, $\varphi = 90.7^\circ$; and (I) $\theta = 1.1^\circ$, no retardation plate. The scenes without the retardation plate are optional for a fully polarimetric calibration, but do improve the calibration accuracy.

IV. CHARACTERISTICS OF THE STANDARD

A. Measurements

To verify the viability of the FPCS, several experiments were conducted to calibrate the Fully Polarimetric Radiometer. Fig. 3 illustrates the calibrated brightness temperature scenes that were generated by the FPCS during a sample calibration. To improve the clarity of the figure, the calibration of the rotation angle θ and the conventional calibrations are not presented. Considering that the calibration of θ requires ~ 2 min in a nominal case, it can be concluded that the generation of the required fully polarimetric brightness temperature scenes can be accomplished within 10 min.

Several tests were carried out to define the characteristics of the FPCS; the results are summarized in Table I. In the tests it was noticed that the lowest brightness temperatures generated by the FPCS (vertical brightness temperature at $\theta = 90^\circ$ and horizontal at $\theta = 0^\circ$) have a warm bias compared to the brightness temperature of a conventional cold blackbody target. After various tests [19], it was concluded that the biases are most probably generated by the nonidealities of the polarizing grid. Modeling the grid characteristics using the warm bias, however, gives somewhat deteriorated values compared to the nearly ideal values presented in [13]. A possible explanation is the relatively low physical temperature of the grid during calibration, which could lead to sacking of the wires; the frame of the grid is made of stainless steel, which has a considerably higher temperature coefficient than the molybdenum wires. This would also explain the different results at $\theta = 0^\circ$ and $\theta = 90^\circ$. Another potential

TABLE I
CHARACTERISTICS OF THE FPCS. ^a WITH THE ROTATION ANGLE OF THE LINEARLY POLARIZED TARGET (θ) 0° AND 90° , RESPECTIVELY. ^b AT 36.5-GHZ CENTER FREQUENCY OVER A 430-MHZ BAND. ^c IN 10, 15, 20, AND 25 min, RESPECTIVELY

Parameter	Value
Power transmission of the polarizing grid, electric field perpendicular to the grid wires ^{a,b} (%)	97.0, 95.7
Power transmission of the polarizing grid, electric field in parallel with the grid wires ^{a,b} (%)	2.0, 3.3
Ohmic losses of the polarizing grid ^b (%)	1.0
Phase shift of the retardation plate ^b (deg)	35.3
Transmission loss of the retardation plate in parallel with the grooves ^b	1.0096 (0.04 dB)
Transmission loss of the retardation plate perpendicular to the grooves ^b	1.0073 (0.03 dB)
Drift of the brightness temperature of the cold target ^c (K)	0.1, 0.35, 0.75, 1.3
Total weight (kg)	28

explanation for the sacking of the wires is the deterioration of the wire bonding.

The weights assigned to the temperature sensors were estimated comparing the evolution of the radiometric responses with the data from the temperature sensors embedded into the hot load of the FPCS. The rotation angle θ was held constant during each measurement. An estimate for the ohmic losses of the grid was obtained comparing the measured brightness temperatures of the hot and cold targets with the physical temperatures determined *a priori*.

Using the radiometer as a reference instrument, the comparison of the tripolarimetric and fully polarimetric brightness

TABLE II
UNCERTAINTIES ASSOCIATED WITH THE PARAMETERS OF THE FPCS

	T_{HOT}	T_{COLD}	θ	L_G	φ	ζ	L_{\parallel}	L_{\perp}	T_R
Random uncertainty	0.15 K	0.15 K	0.1°	-	0.2°	-	-	-	3 K
Systematic uncertainty	0.2 K	0.5 K	0.1°	0.003	0.2°	0.2°	$9 \cdot 10^{-4}$	$8 \cdot 10^{-4}$	5 K

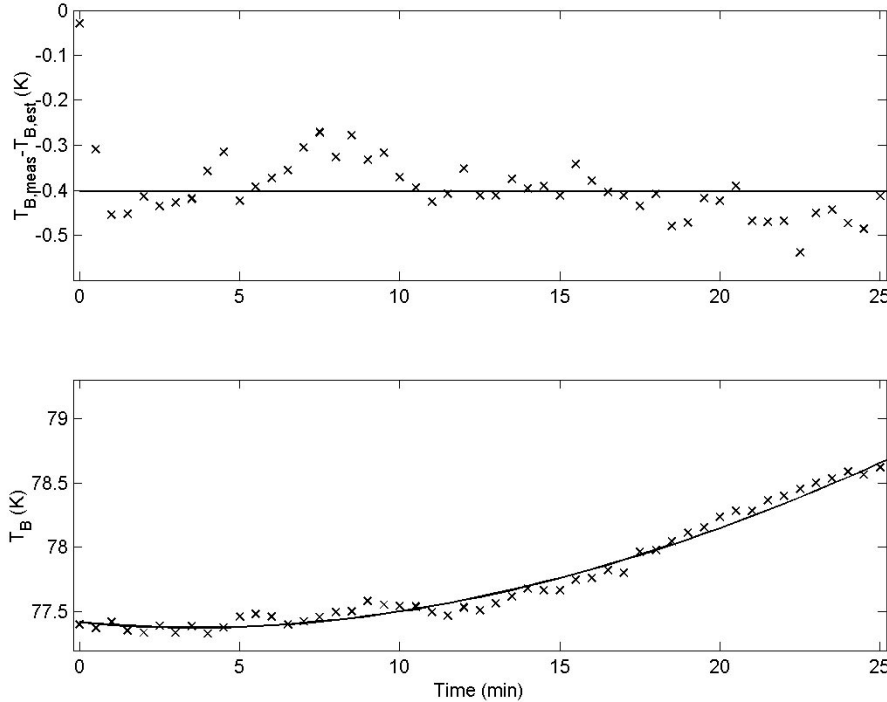


Fig. 4. Difference between (top) the measured and estimated brightness temperatures of the hot blackbody target and (bottom) the evaluation of the brightness temperature of the cold blackbody target of the FPCS as a function of time. The solid line in the top indicates an offset of 0.4 K, while the solid line in the bottom indicates a third-order polynomial regression curve.

temperature scenes enabled the definition of the characteristics of the phase retardation plate. The insertion loss of the plate, parallel and perpendicular to the grooves, was measured to be 1.0096 ($=0.04$ dB) and 1.0073 ($=0.03$ dB), respectively, which are very close to the theoretical values presented in Section II-C. The high repeatability of the results—the standard deviations are 0.0009 and 0.0008 for the parallel and perpendicular case, respectively—indicates that the retardation plate is well matched at the applied frequency band. The phase shift of the plate was measured to be 35.3° , which deviates somewhat from the theoretical value of 37.0° . Possible explanations are machining tolerances and the uncertainties in estimating the dielectric constant of Rexolite. A small misalignment of 0.7° between the coordinate axes of the retardation plate and the antenna polarization basis was also identified in these measurements; this misalignment is accounted for in calculating *a priori* brightness temperature of the fourth Stokes parameter, which significantly improves the calibration accuracy. Note also that active methods, as described, for example, in [17], could be applied to determine the characteristics of the retardation plate.

B. Error Analysis

The uncertainties associated with the fully polarimetric calibration generate errors in the retrieved brightness temperature.

To study the calibration errors when calibrating the Fully Polarimetric Radiometer with the FPCS, the uncertainties of the individual calibration standard parameters were studied. The individual uncertainties are summarized in Table II. Random and systematic uncertainty parameters are listed separately as the influence of the systematic uncertainties could be reduced *a posteriori*, as discussed in [10].

The brightness temperature of the cold target of the FPCS is defined to be constant *a priori*; a drift is thus a potential (random) error source if not compensated for in postprocessing. As presented in Fig. 4, the stability of the cold target was studied by measuring the evolution of the radiometric response as a function of time. The rotation angle θ was set to 0° to minimize the mixing of brightness temperatures. Note that the influence of the polarizing grid has been removed. To reduce the influence of the radiometer noise, the behavior is modeled using a third-order polynomial fit. Numerical estimates for the drift are given in Table I. It can be concluded that the drift is small (≤ 0.1 K) over time periods required for a fully polarimetric calibration ~ 10 min. Note that this measurement gives a somewhat conservative estimate for the stability; it has been observed that the rotation of the cold target subsystem during a calibration effectively reduces the temperature increase. Thus, the temperature increase can be neglected for time scales ≤ 10 min.

The random error in determining the brightness temperature of the hot load was studied in the same measurement described above. During the measurement the physical temperature of the hot target changed ~ 18 K; Fig. 4 presents the difference between the measured brightness temperature and the brightness temperature determined *a priori* using the temperature sensor data and the predetermined sensor weights. The results indicate that using the temperature sensors the determination of the brightness temperature is feasible and fairly accurate; omitting an 0.4-K offset, the standard deviation of the difference is only 0.06 K, which is not significantly higher than the radiometric sensitivity of the data, 0.04 K. Increasing the number of temperature detectors and/or determining more accurately the weights of the temperature sensors would probably suppress the offset. Note, however, that the isolation of the orthogonal channels of the Fully Polarimetric Radiometer has been found to be -30 dB at minimum [8], which can be used beneficially to improve calibration accuracy; the calibration coefficients of the orthogonal channels can now be retrieved using just the unpolarized calibration scenes. Furthermore, using conventional hot–cold calibration as a reference, this *a priori* knowledge of the radiometer characteristics (and the fact that the sum of orthogonal brightness temperatures is for all values of θ very close to the sum of the brightness temperatures of the hot and cold targets) makes it possible to estimate T'_{HOT} and T'_{COLD} (which include the influence of the polarizing grid; see [10]) during tripolarimetric calibration configurations. The calibration coefficients of the third Stokes parameter, except the cross-talk between the two polarimetric channels, can therefore be determined without using the temperature sensor data and the reflection and transmission characteristics of the grid. Applying the temperature sensor data to compensate the temperature excursions of T'_{HOT} between the tripolarimetric and fully polarimetric calibration scenes, the calibration coefficients of the fourth Stokes parameter (and the remaining coefficient of the third parameter) can also be calibrated with enhanced accuracy. The uncertainty in compensating the temperature excursions of T'_{HOT} was set conservatively to 0.2 K.

To estimate the random uncertainties associated with the conventional calibrations, a series of 18 separate hot–cold calibrations were conducted. It was noticed that, compared to a single two-point calibration, the use of multiple calibrations suppressed the uncertainties significantly; 0.1-K random uncertainty seems to be achievable in laboratory conditions for both hot and cold calibrations if the calibration is repeated six times. In field conditions, however, the influence of wind, the sun, and other factors may increase the calibration uncertainties, and a random uncertainty of 0.15 K is probably a more realistic estimate.

The method used to determine the applied rotation angle θ in the vicinity of 0° and 90° was described in Section III-B; an accurate value of θ in the vicinity of 45° can be found by comparing the observed orthogonal brightness temperatures. During the processing of calibration data, the overdetermination of the \overline{C}_0 -matrix in (4) makes it possible to enhance the accuracy to a predicted value of 0.1° . The random uncertainty of the rotation angle φ was measured to be 0.2° .

Systematic uncertainty in determining the physical temperature of the conventional hot blackbody target is largely defined by the accuracy of the thermometer. To determine the temperature in each of the six hot–cold calibrations, a hand-held electronic thermometer is applied; the electronic thermometer is in turn calibrated using a mercury thermometer as a reference standard. Taking into account the unknown temperature distribution of the hot target, the uncertainty is predicted to be 0.2 K. The physical temperature of the cold target is obtained *a priori* from the boiling temperature of nitrogen in the given atmospheric pressure. The estimation of the systematic uncertainty is non-trivial, though; we predict that a cold calibration—if done carefully—can provide the brightness temperature with a systematic uncertainty of 0.5 K.

The losses and the phase shift of the retardation plate were determined by comparing the results obtained by tripolarimetric and fully polarimetric calibration scenes. The uncertainties of the obtained values, which represent systematic errors for fully polarimetric calibrations, were defined as standard deviations of results from several measurements. The systematic uncertainties in determining the rotation angle θ and φ are predicted to be equal to random uncertainties (0.1° and 0.2° , respectively), and the uncertainty in determining the ohmic losses of the polarizing grid (L_G) was set to 0.003.

C. Uncertainties in Wind Vector Measurements

One promising application of the polarimetric microwave radiometers is the determination of maritime wind vectors (e.g., see [2]–[5]). The applicability of our system for wind vector retrieval was also studied as described in [10]; calibration uncertainties were studied for a simulated oceanic brightness temperature scene assuming a 53° incidence angle, a sea surface temperature of 4.6°C , and wind speed of 5 ms^{-1} . It is further assumed that both tripolarimetric and fully polarimetric calibration scenes are applied in calibration and the *a priori* knowledge of the radiometer characteristics, discussed earlier, is used. Both random and systematic uncertainties of the FPCS, presented in Table II, were considered, as well as the uncertainties of the radiometer parameters that were estimated *a priori* (-30 dB [8]).

The estimated total errors in the sample wind vector measurement are 0.4 and 0.6 K for T_v and T_h , respectively, and 0.4 and 0.8 K for T_3 and T_4 , respectively. These estimates are also in line with experimental results presented in [8]. Note, however, that the calibration errors caused by systematic uncertainties can be compensated for *a posteriori* at least in part [10]. Considering only the random parameter uncertainties of the FPCS, the estimated generated measurement error is 0.1 K for orthogonal polarizations and 0.3 and 0.5 K for T_3 and T_4 , respectively. In both cases, the most significant error sources are the inaccuracies in determining the brightness temperatures of the unpolarized targets and in determining the rotation angles θ and φ of the FPCS. For systematic uncertainties, the inaccuracies in determining the radiometer characteristics *a priori* are also significant.

According to [20], the sensitivity of the vertical brightness temperature to wind speed is $\sim 1.6\text{ Km}^{-1}\text{s}$ or higher. The estimated random and systematic uncertainties of the FPCS parameters thus suggest a wind speed measurement inaccuracy of

0.25 ms⁻¹. Compensating for the systematic uncertainties or using *in situ* reference data can potentially improve the accuracy further.

As is discussed in [10], the high accuracy in pixel-to-pixel wind direction retrieval requires an extremely high absolute calibration accuracy of T_3 : for a wind speed of 10 ms⁻¹, for example, an inaccuracy of 20° would require an absolute calibration accuracy of 0.24 K at 37 GHz. This threshold, however, can be relaxed using the whole Stokes vector for determining the wind direction. Furthermore, additional methods can be applied to improve the wind direction retrieval, e.g., circle flights [3]: the averaged value of T_3 and T_4 over all relative wind directions should be zero, and the residual bias terms can be removed. Another option is cross-calibration with other instruments.

V. CONCLUSION

This paper describes the Helsinki University of Technology's Fully Polarimetric Calibration Standard, which is a passive structure that provides a set of precisely known fully polarimetric brightness temperature scenes for the end-to-end calibration of the HUT Fully Polarimetric Radiometer [8]. The radiometer operates at 36.5 GHz, and it is designed primarily for airborne earth remote sensing. However, laboratory and ground-based measurements are also foreseen; the FPCS was thus designed for versatile operation in the laboratory, airport, and other field conditions (e.g., on rooftops). The functional and ergonomic requirements were met using a modular structure, which allowed the combination of high calibration accuracy with easy transport, mobilization, and operation; a single operator can take care of the whole calibration process, if necessary. The developed calibration standard is based on a tripolarimetric standard, the function principle of which was described in [12], with an additional phase retardation plate to generate the fourth Stokes parameter.

The function of the FPCS and the applicability of the calibration procedure are demonstrated. As the retardation plate is easily attached and detached, an advanced calibration procedure with the generation of both tripolarimetric and fully polarimetric brightness temperature scenes can be applied to suppress calibration uncertainties. It was demonstrated that the procedure also enables the accurate determination of retardation plate characteristics.

A variety of laboratory tests were performed to define the characteristics of the FPCS and the associated uncertainties. The influence of the calibration errors in a potential wind vector measurement was also analyzed. Calibrating the Fully Polarimetric Radiometer with the developed standard, the estimated absolute accuracy of the measured Stokes vector is very high; to the authors' knowledge, these values are the best reported so far for a fully polarimetric calibration standard. The calibration accuracy presented here allows the retrieval of the wind speed with high accuracy and the retrieval of the wind direction with moderate accuracy. To enhance the accuracy of the wind direction retrieval, additional calibration methods (e.g., circle flights [3]) can be considered.

The described standard was developed to determine the calibration coefficients of a fully polarimetric radiometer. How-

ever, tripolarimetric radiometers (that measure only three Stokes parameter) would also benefit from the determination of the phase balance between orthogonal channels, which cannot be performed using a tripolarimetric calibration standard; the imperfect phase balance leads to mixing of the third and fourth Stokes parameters if it is not compensated for in software. A potential application of the FPCS is also the determination of the channel cross-talk of conventional radiometers, which can lead to measurement error on targets with distinct brightness temperatures at vertical and horizontal polarizations, such as water. Furthermore, the developed standard generates adjustable brightness temperatures and can be applied to measure the non-linearity of a receiver by generating multiple reference brightness temperatures and using them as calibration points. The measurement of this nonlinearity is an indirect but potentially useful application of the developed standard; the receiver non-linearity can be up to some Kelvin [21] but is frequently overlooked as an error source in a conventional two-blackbody calibration scheme. As the FPCS applies integrated blackbody targets at ambient and boiling nitrogen temperatures, the generated Stokes vectors allow the measurement of the receiver linearity practically over the whole range of terrestrial brightness temperatures.

ACKNOWLEDGMENT

The authors wish to thank the following individuals for their help in the design and fabrication of the calibration standard: P. Rummukainen, M. Kemppinen, S. Ruokolainen, and H. Äyhynmäki. Further, the valuable contribution of M. Roschier in the design of the pedestal is gratefully acknowledged, as are the valuable suggestions made by J. Pulliainen.

REFERENCES

- [1] L. Tsang, J. A. Kong, and R. T. Shin, *Theory of Microwave Remote Sensing*. New York: Wiley, 1985.
- [2] M. S. Dzura, V. S. Etkin, A. S. Khrupin, M. N. Pospelov, and M. D. Raev, "Radiometers-polarimeters: Principles of design and application for sea surface microwave emission polarimetry," in *Proc. IGARSS*, 1992, pp. 1432–1434.
- [3] S. H. Yueh, W. J. Wilson, F. K. Li, S. V. Nghiem, and W. B. Ricketts, "Polarimetric brightness temperatures of sea surfaces measured with aircraft K- and Ka-band radiometers," *IEEE Trans. Geosci. Remote Sensing*, vol. 35, pp. 1177–1187, Sept. 1997.
- [4] J. R. Piepmeier and A. J. Gasiewski, "High-resolution passive polarimetric microwave mapping of ocean surface wind vector fields," *IEEE Trans. Geosci. Remote Sensing*, vol. 39, pp. 606–622, Mar. 2001.
- [5] B. Laursen and N. Skou, "Wind direction over ocean determined by an airborne, imaging, polarimetric radiometer system," *IEEE Trans. Geosci. Remote Sensing*, vol. 39, pp. 1547–1555, July 2001.
- [6] P. W. Rosenkranz and D. H. Staelin, "Polarized thermal microwave emission from oxygen in the mesosphere," *Radio Sci.*, vol. 23, pp. 721–729, Sept.–Oct. 1988.
- [7] M. Hallikainen, M. Kemppinen, J. Pihlflyckt, I. Mononen, T. Auer, K. Rautiainen, and J. Lahtinen, "HUTRAD: Airborne multifrequency microwave radiometer," in *Proc. ESA Workshop on Millimeter Wave Technology and Applications: Antennas, Circuits and Systems*, 1998, pp. 115–120.
- [8] J. Lahtinen, J. Pihlflyckt, I. Mononen, S. Tauriainen, M. Kemppinen, and M. Hallikainen, "Fully polarimetric microwave radiometer for remote sensing," *IEEE Trans. Geosci. Remote Sensing*, 2003, to be published.
- [9] O. Koistinen, J. Lahtinen, and M. Hallikainen, "Comparison of analog continuum correlators for remote sensing and radio astronomy," *IEEE Trans. Instrum. Meas.*, vol. 51, pp. 227–234, Apr. 2002.

- [10] J. Lahtinen, A. J. Gasiewski, M. Klein, and I. Corbella, "A calibration method for fully polarimetric microwave radiometers," *IEEE Trans. Geosci. Remote Sensing*, vol. 41, pp. 588–602, Mar. 2003.
- [11] J. Lahtinen and M. Hallikainen, "Fully polarimetric calibration system for HUT polarimetric radiometer," in *Proc. IGARSS*, 2000, pp. 1542–1544.
- [12] A. J. Gasiewski and D. B. Kunkee, "Calibration and application of polarization-correlating radiometers," *IEEE Trans. Microwave Theory Tech.*, vol. 41, pp. 767–773, May 1993.
- [13] J. Lahtinen and M. Hallikainen, "Fabrication and characterization of large free-standing polarizer grids for millimeter waves," *Int. J. Inf. Millim. Waves*, vol. 20, no. 1, pp. 3–20, Jan. 1999.
- [14] W. N. Hardy, "Precision temperature reference for microwave radiometry," *IEEE Trans. Microwave Theory Tech.*, vol. MTT-21, pp. 149–150, Mar. 1973.
- [15] Radiometrics Corp., Boulder, CO, Tech. Memo. 6/22/94, 1994.
- [16] A. H. F. van Vliet and T. de Graauw, "Quarter wave plates for sub-millimeter wavelengths," *Int. J. Inf. Millim. Waves*, vol. 2, no. 3, pp. 465–477, 1981.
- [17] J. W. Lamb, A. V. Räisänen, and M. A. Tiuri, "Feed system for the Metsähovi cooled 75–95 GHz receiver," Helsinki Univ. Technol., Radio Lab., Espoo, Finland, Rep. S 146, 1983.
- [18] F. I. Shimabukuro and C. Yeh, "Attenuation measurement of very low loss dielectric waveguides by the cavity resonator method applicable in the millimeter/submillimeter wavelength range," *IEEE Trans. Microwave Theory Tech.*, vol. 36, pp. 1160–1166, July 1988.
- [19] J. Lahtinen, "Calibration system for fully polarimetric microwave radiometers," Licentiate thesis, Helsinki Univ. Technol., Dept. Elect. Telecommun. Eng., Espoo, Finland, 2001.
- [20] F. J. Wentz, "Measurement of oceanic wind vector using satellite microwave radiometer," *IEEE Trans. Geosci. Remote Sensing*, vol. 30, pp. 960–972, Sept. 1992.
- [21] S. Kazama, T. Rose, R. Zimmermann, and R. Zimmermann, "A precision autocalibrating 7 channel radiometer for environmental research applications," *J. Remote Sens. Soc. Jpn.*, vol. 19, no. 3, pp. 37–45, 1999.



Janne Lahtinen (S'98) received the M.S. (Tech.) and Lic. Sci. (Tech.) degrees from the Helsinki University of Technology (HUT), Espoo, Finland, in 1996 and 2001, respectively.

He is currently a Research Fellow at the European Space Agency's European Research and Technology Centre (ESTEC), Noordwijk, The Netherlands. From 1995 to 2002, he was with the HUT Laboratory of Space Technology. His research has focused on microwave radiometer systems, with emphasis on polarimetric and interferometric radiometers. He has

authored and coauthored more than 20 publications in the area of microwave remote sensing.

Mr. Lahtinen received the third place in the IEEE Geoscience and Remote Sensing Society Student Prize Paper Competition in 2000, and he won the Young Scientist Award of the Finnish National Convention on Radio Science in 2001. He served as a Secretary of the Finnish National Committee of COSPAR from 1997 to 2002 and as a Secretary of the Space Science Committee, appointed by Finnish Ministry of Education, from 1999 to 2000.



Martti T. Hallikainen (M'83–SM'85–F'93) received the M.S. degree in engineering and the Dir. Tech. degree from the Faculty of Electrical Engineering, Helsinki University of Technology (HUT), Espoo, Finland, in 1971 and 1980, respectively.

Since 1987, he has been a Professor of Space Technology at HUT, where his research interests include remote sensing and satellite technology. In 1988, he established the HUT Laboratory of Space Technology and serves as its Director. He was a Visiting Scientist from 1993 to 1994 at the European

Union's Joint Research Centre, Institute for Remote Sensing Applications, Ispra, Italy. He was a Postdoctoral Fellow at the Remote Sensing Laboratory, University of Kansas, Lawrence, from 1981 to 1983, and was awarded an ASLA Fulbright Scholarship for graduate studies at the University of Texas, Austin, in 1974–1975. He is an author/coauthor of over 500 scientific publications.

Dr. Hallikainen served as President of IEEE Geoscience and Remote Sensing Society (IEEE GRSS) in 1996 and 1997, and as Vice President in 1994 and 1995. Since 1988, he has been a member of the IEEE GRSS Administrative Committee, and from 1999 to 2001, he served as the IEEE GRSS Nominations Committee Chair and since 2002, as the Fellow Search Committee Chair. He was the General Chairman of the IGARSS'91 Symposium and Guest Editor of the Special IGARSS'91 Issue of the IEEE TRANSACTIONS ON GEOSCIENCE AND REMOTE SENSING (TGARS). Since 1992, he has been an Associate Editor of TGARS. He was a member of the IEEE Periodicals Committee in 1997 and Corresponding member of the IEEE New Technology Directions Committee from 1992 to 1995. He was Secretary General of the European Association of Remote Sensing Laboratories (EARSeL) from 1989 to 1993 and Chairman of the Organizing Committee for the EARSeL 1989 General Assembly and Symposium. He has been a member of the EARSeL Council since 1985, and he was a member of the Editorial Board of the EARSeL Advances in Remote Sensing from 1992 to 1993. He has been a member of the European Space Agency's (ESA) Earth Science Advisory Committee since 1998 and a member of the ESA SMOS Scientific Advisory Group since 2000. He was a national delegate to the ESA Earth Observation Scientific and Technical Advisory Group (EOSTAG) from 1988 to 1994, and he has served in the same capacity on the ESA Earth Observation Data Operations Scientific and Technical Advisory Group (DOSTAG) since 1995. He was Thematic Coordinator of the ESA EMAC-95 airborne campaign for Snow and Ice activities. He was a member of the ESA Multi-frequency Imaging Microwave Radiometer (MIMR) Expert Group from 1988 to 1994 and was a member of the ESA MIMR Scientific Advisory Group from 1994 to 1996. Since 1992, he has been a member of both the Advisory Committee for the European Microwave Signature Laboratory of the European Union's Joint Research Centre and the National Liaison of the International Space University. He is currently serving as Chair of Commission F International Union of Radio Science (URSI) from 2002 to 2005 and has served as its Vice Chair from 1999 to 2002. He was a member of the URSI Long Range Planning Committee from 1996 to 1999, a member of the URSI Committee on Geosphere and Biosphere Program from 1989 to 1999, and a URSI representative to SCOR from 1999 to 2002. He has been a national official member of URSI Commission F (Wave Propagation and Remote Sensing) since 1988. He was Secretary of the Organizing Committee for the URSI Nordic Antenna Symposium in 1976, and he served as Secretary of the Finnish National Committee of URSI from 1975 to 1989. He was Vice Chair of the URSI Finnish National Committee from 1990 to 1996, and he has served as its Chair since 1997. He is Vice Chair of the Finnish National Committee of COSPAR since 2000. He is the recipient of three IEEE GRSS Awards: 1999 Distinguished Achievement Award, IGARSS'96 Interactive Paper Award, and 1994 Outstanding Service Award. He is the winner of the Microwave Prize for the best paper in the 1992 European Microwave Conference, and he received the HUT Foundation Award for excellence in research in 1990. He and his research team received the 1989 National Research Project of the Year Award from *Tekniikka & Talous (Technology & Management Magazine)*. He received the 1984 Editorial Board Prize of Sähkö—Electricity in Finland.